Journal of Bioscience and Bioengineering
VOL. 107 No. 1, 90 – 94, 2009

ELSEVIER

www.elsevier.com/locate/jbiosc

Classification of pollen species using autofluorescence image analysis

Kotaro Mitsumoto,[1,2] Katsumi Yabusaki,[1,*] and Hideki Aoyagi[2]

Electronics and Optics Research Laboratories, Kowa Company, Ltd., 3-3-1 Chofugaoka, Chofu, Tokyo 182-0021, Japan[1] *and Life Science and Bioengineering, Graduate School of Life and Environmental Sciences, University of Tsukuba, 1-1-1 Tennodai, Tsukuba, Ibaraki 305-8572, Japan*[2]

Received 20 February 2008; accepted 27 October 2008

A new method to classify pollen species was developed by monitoring autofluorescence images of pollen grains. The pollens of nine species were selected, and their autofluorescence images were captured by a microscope equipped with a digital camera. The pollen size and the ratio of the blue to red pollen autofluorescence spectra (the B/R ratio) were calculated by image processing. The B/R ratios and pollen size varied among the species. Furthermore, the scatter-plot of pollen size versus the B/R ratio showed that pollen could be classified to the species level using both parameters. The pollen size and B/R ratio were confirmed by means of particle flow image analysis and the fluorescence spectra, respectively. These results suggest that a flow system capable of measuring both scattered light and the autofluorescence of particles could classify and count pollen grains in real time.

[**Key words:** Pollen; Pollen counting; Pollen classification; Autofluorescence; Microscopic image analysis; Hay fever]

Millions of people in Japan suffer from seasonal pollen allergies, commonly referred to as “hay fever” accompanied by several symptoms like sneezing, itchiness, a runny nose, and watering eyes during periods each spring when the pollen of Japanese cedar (*Cryptomeria japonica*) and Japanese cypress (*Chamaecyparis obtusa*) are suspended in the air. Accurate, reliable, and timely information about the quantity of airborne pollen can greatly help hay fever patients to manage their symptoms and daily life. Conventional approaches have counted airborne pollen grains manually under a microscope. For example, the Durham method has been widely adopted in Japan to quantify the density of airborne pollen (1). In Europe, the Burkard volumetric sampler has been used to collect airborne pollen grains (2). Although both methods are easy to introduce to researchers, identifying and counting pollen grains under the microscope are demanding and time-consuming tasks, even for experienced microscopists. Pollen grains show strong autofluorescence (3). According to Pinnick et al., fluorescence is a useful index to distinguish between biological and non-biological airborne particles (4); thus fluorescence microscopy is a practical technique for the investigation of pollen grains (5–7). Fluorescence microscopy is currently demonstrating great potential for qualitative and quantitative studies of the structure and function of plant cells, since fluorescence from a single cell can be detected both as an image and as a photometric signal (8, 9). Recent advances in the instruments used for acquiring, processing, and analyzing fluorescence signals have now made it possible to classify and count pollen grains. Ronneberger et al. reported that a system based on the 3D volumetric fluorescence image of a pollen grain taken with a confocal laser scanning microscope was able to recognize pollen taxa with a recognition rate of more than 90% (7). This method, however, was not suitable for counting airborne pollen grains in real time.

We considered that one of the most useful procedures for automatically classifying and counting airborne particles in real time involves the use of a flow system such as flow cytometry, which is based on measuring the fluorescence and light scattered from cells. So, in this study, we analyzed microscopic autofluorescence images of pollen grains from several species and found that they could be distinguished based on the characteristics of their autofluorescence spectra and particle sizes.

MATERIALS AND METHODS

Pollen grain samples Nine plant species were selected for this study: *C. japonica*, *C. obtusa*, *Betula mandshurica* var. *japonica*, *Dactylis glomerata*, *Ambrosia artemisiaefolia* var. *elatior*, *Artemisia princeps*, *Fagus crenata*, *Cynodon dactylon*, and *Sorghum halepense*. Pollen samples were kindly provided by Dr. Yuichi Takahashi (Yamagata Prefectural Institute of Public Health, Japan).

Microscopic fluorescence image analysis Fluorescence and bright-field images of pollen grains on a glass plate were observed with a biological fluorescent microscope (IMT-2, Olympus, Tokyo) equipped with a 20× objective lens and ultraviolet illuminating system using a xenon lamp and a band-pass filter (central wavelength: 340 nm). Digital images of them were captured with a three-shot single-chip charge-coupled device (CCD) camera (SPOT ISA-CE Color, Diagnostic Instruments Inc., Sterling Heights, MI, USA) connected to the microscope, and the resulting data were stored in a personal computer. The CCD camera has three movable color filters (blue, green, and red) in front of the detectors so that the sensors can receive images sequentially and save precise data for each color wavelength. The captured images were analyzed using a Photoshop image-processing and -analyzing software (Adobe Systems, San Jose, CA, USA) to provide the average red, green, and blue pixel values for the fluorescence intensity of each of 15 pollen grains selected in an image. In this analysis, we simulated a

* Corresponding author. Tel.: +81 29 836 4611; fax: +81 29 836 4609.
E-mail address: yabusaki@kowa.co.jp (K. Yabusaki).

1389-1723/$ - see front matter © 2008, The Society for Biotechnology, Japan. All rights reserved.
doi:10.1016/j.jbiosc.2008.10.001

pollen grain as a perfect sphere, with a circular surface, and converted the area into a diameter using the formula $area = \pi r^2$.

Measurement of the fluorescence spectrum The fluorescence spectra of the pollen grains were measured using a C2741-08 digital camera (Hamamatsu Photonics, Shizuoka, Japan) equipped with a VariSpec electronically tunable liquid-crystal filter (CRI Inc., Woburn, MA, USA), which freely changes the transmittable wavelength. The filter and digital camera were mounted on the microscope, and then pollen grains were illuminated by using a xenon lamp and a band-pass filter (central wavelength: 380 nm). Fluorescence images were captured through the tunable filter at 10-nm intervals in the wavelength range from 400 to 700 nm. The fluorescence intensities of each species were calculated with normalization against the background fluorescence intensity, where no pollen grains were localized. The averaged fluorescence intensities of ten pollen grains were plotted against the emitted wavelength for each species. To derive the B/R ratios, the values of area under the curve (AUC) for the fluorescence spectra were calculated by summing the fluorescence intensity. Fluorescence from 400 to 550 nm was determined as blue fluorescence and that of from 560 to 700 nm was determined as red fluorescence.

Flow image analysis Size and shape of particles were measured in a fluid flow using its sheath-flow cell system, which positions the particles within the same focal plane (FPIA-3000, Sysmex Corporation, Kobe, Japan). A strobe light illuminates the particles as they pass through the measurement cell, and their images are captured by a digital camera. The particle size and shape are determined using the attached image-analysis software. The size of a particle is calculated from the diameter of a circle with the same area as an objective particle. In this study, we used the number-weighted diameter to compare the diameter obtained from the microscopic image analysis and particles ranging from 0.25 to 400 μm in size were analyzed. The shape of a particle is expressed by the circularity, which means how the shape of a particle is close to a circle. In this software, the circularity is defined as the ratio of the perimeter of a circle with same area as a particle to the actual perimeter of a particle. Therefore the circularity is expressed by $C = 2\sqrt{\pi S}/A_p$, where C is the circularity, S is the area of a particle, and A_p is the actual perimeter of a particle. As the shape of particle approaches to a perfect circle, the circularity becomes 1.0. In this analysis, representative four allergenic pollens in Japan were measured. Pollen grains suspended in isopropyl alcohol (2.0 mg/ml) were used for measurement to avoid the destruction of pollen cell wall.

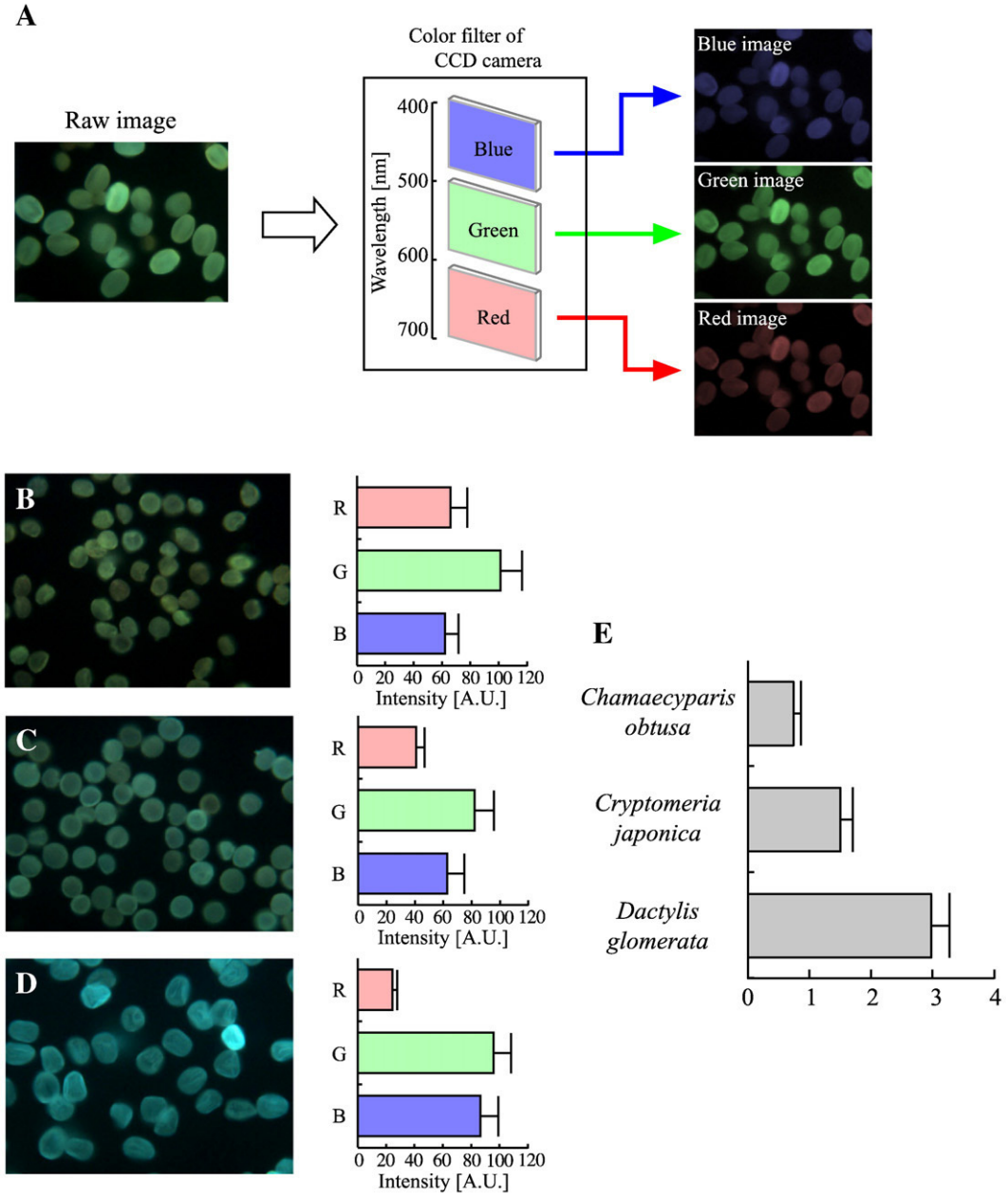

FIG. 1. Quantification of pollen autofluorescence. (A) Fluorescence images captured using the three-shot single-chip CCD camera. Fluorescence from pollen grains was captured sequentially through blue, green, and red color filters. (B), (C), and (D) Fluorescence images of (left) *Chamaecyparis obtusa*, *Cryptomeria japonica*, and *Dactylis glomerata* pollen grains and (right) the corresponding RGB pixel values. (E) Blue to red (B/R) fluorescence ratio of the three species. Range bars show the standard deviation (SD) of the mean value for 15 pollen grains.

Particle size analysis by means of scattering of laser light The sizes of the pollen grains were also measured in the gas line using Mastersizer 2000 particle size analyzer (Malvern Instruments Ltd., Worcestershire, UK). Mean size and dispersion of particles were quantified based on the diffraction and scattering of laser light under dry measurement conditions. A helium-neon laser at 633 nm and a blue light-emitting diode (LED) at 466 nm provide the illumination, and the particle sizes are analyzed based on the principle of Mie theory (10). The device is capable of measuring particles ranging in size from 0.02 to 2000 μm. Pollen grains dispersed in dry air were used for this measurement.

RESULTS

Microscopic fluorescence image analysis We studied pollen grains from nine species. Representative fluorescence images are shown in Fig. 1. Most species of pollen grains showed strong green fluorescence, but also exhibited significant blue and red fluorescence (Figs. 1A–D). To quantify the red, green, and blue fluorescence intensities, the pixel values of each color in the pollen images were averaged. This quantification revealed that the ratio of the intensity of the three fluorescence colors varied among the species. *C. obtusa*, for instance, showed similar intensities of red and blue fluorescence (Fig. 1B). In contrast, *C. japonica* and *D. glomerata* showed higher green and blue fluorescence intensities (Figs. 1C, D). Based on the observed differences, the ratios of blue to red fluorescence intensity (the B/R ratio) were calculated for these species (Fig. 1E). The B/R ratios of *C. obtusa*, *C. japonica*, and *D. glomerata* were 0.74, 1.50, and 2.97, respectively. The B/R ratios of the other species are shown in Fig. 2.

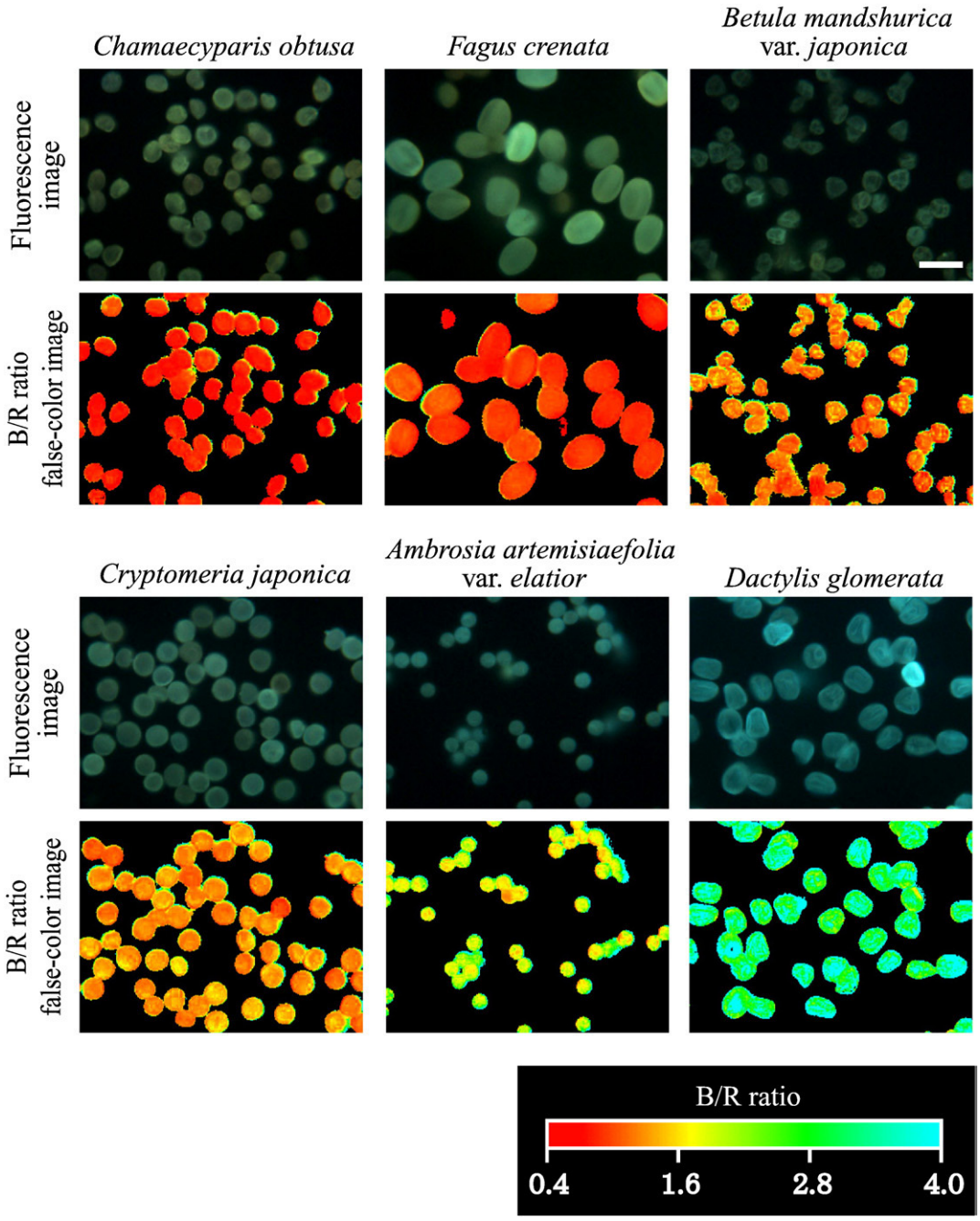

FIG. 2. Fluorescence images and false-color images of the B/R ratio of the pollen grains. B/R ratios ranging from 0.4 to 4.0 were represented using colors from red to blue, respectively. The scale bar in the image equals 50 μm.

To assess variations in the B/R ratio among species, false-color B/R ratio images were displayed below the fluorescence images (Fig. 2). B/R ratios ranging from 0.4 to 4.0 were represented using colors ranging from red to blue, respectively. The false-color images clearly showed that the B/R ratio varied among the species. For example, *C. obtusa* and *F. crenata* had a strong red color, and *D. glomerata* had a strong blue-green color. The mean B/R ratios of the 15 pollen grains of each species are shown in Table 1. The B/R ratio of *F. crenata* was significantly greater than that of *C. obtusa* ($P<0.05$, *t*-test), but not different from those of *B. mandshurica* var. *japonica* and *S. halepense*. On the other hand, the mean size of *F. crenata* pollen grains was significantly greater than that of *B. mandshurica* var. *japonica* and *S. halepense* (Table 1). These results thus indicate that the size of the pollen grains and their B/R ratio differ among the species and are important parameters that can be used to classify pollen to the species level.

Fig. 3 represents the relationship between the grain diameter and B/R ratio of the pollen grains. The results show that values for the pollen grains of a given species tended to cluster within a limited area of the graph. Even though *F. crenata* and *B. mandshurica* var. *japonica* had similar B/R ratios, they differed sufficiently in grain diameter that pollen of the two species formed distinct groups in the graph. On the other hand, *C. japonica* and *Chamaecyparis obtuse*, which had similar grain sizes, also differed in B/R ratio and formed distinct groups in the graph.

Measurement of the fluorescence spectra Measurements of the pollen fluorescence spectra confirmed the B/R ratios obtained from the fluorescence images using the three-shot single-chip CCD camera. *C. japonica* and *C. obtusa* had spectral peaks at 540 and 570 nm, respectively (Fig. 4). The AUCs for blue and red fluorescence from *C. japonica* were 5.84 and 4.30, respectively. Similarly, the AUCs for blue and red fluorescence from *C. obtusa* were 5.07 and 6.07, respectively. The B/R ratio for *C. japonica* was 1.36, in contrast to 0.84 for *C. obtuse*.

Flow image analysis Size of pollen was measured in real time by the flow system using the particle flow image analyzer (Table 2). The mean size of the pollen grains was 26.0 μm for *C. japonica*, 24.0 μm for *C. obtusa*, 31.7 μm for *D. glomerata*, and 20.7 μm for *A. artemisiaefolia* var. *elatior*, respectively. Although the pollen sizes measured in this way were smaller than those obtained by the microscopic image analysis, the differences were not large. The circularities of the pollen grains were all greater than 0.90. *C. japonica* and *A. artemisiaefolia* var. *elatior* had the greatest circularity values for pollen grains (0.99), whereas *D. glomerata* had the lowest (0.92).

Particle size analysis by means of scattering of laser light For real-time airborne particle counting, the principle of a particle counter is preferable. The mean size of the pollen grains was 26.0 μm for *C. japonica*, 24.1 μm for *C. obtusa*, 34.1 μm for *D. glomerata*, and 21.1 μm for *A. artemisiaefolia* var. *elatior*.

Table 1. Mean pollen diameters and the ratio of blue to red fluorescence (the B/R ratio) for the pollen of nine species investigated by means of microscopic fluorescence image analysis

Species	Diameter [μm]	B/R ratio
Dactylis glomerata	34.7±1.97[b]	2.97±0.26[a]
Ambrosia artemisiaefolia var. *elatior*	21.2±0.94[e]	2.59±0.49[b]
Cynodon dactylon	26.6±1.72[d]	2.45±0.26[b]
Artemisia princeps	20.2±1.91[e]	2.44±0.56[b]
Cryptomeria japonica	29.7±2.26[c]	1.50±0.17[c]
Sorghum halepense	33.1±2.31[b]	1.05±0.18[d]
Betula mandshurica var. *japonica*	25.3±1.57[d]	1.05±0.09[d]
Fagus crenata	42.6±3.83[a]	1.01±0.10[d]
Chamaecyparis obtusa	26.9±3.11[d]	0.74±0.13[e]

Each value represents the mean of 15 pollen grains±SD.
Mean values in a column followed by different letter differ significantly (*t*-test, $P<0.05$).

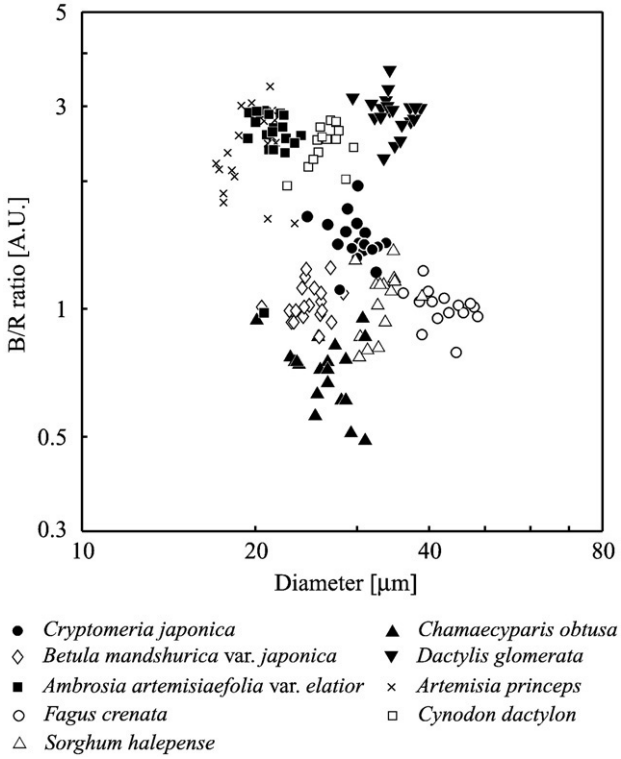

FIG. 3. Graph of the blue to red fluorescence ratio (the B/R ratio) as a function of pollen diameter.

DISCUSSION

The present study revealed that the pollen autofluorescence B/R ratios varied among the species. *C. japonica* and *C. obtusa* are the most familiar and allergenic spring pollen in Japan, and their B/R ratios differed significantly. This result shows that pollen of the two species can be differentiated based on their B/R ratios alone. Ronneberger et al. proposed the use of an automated pollen recognition system based on

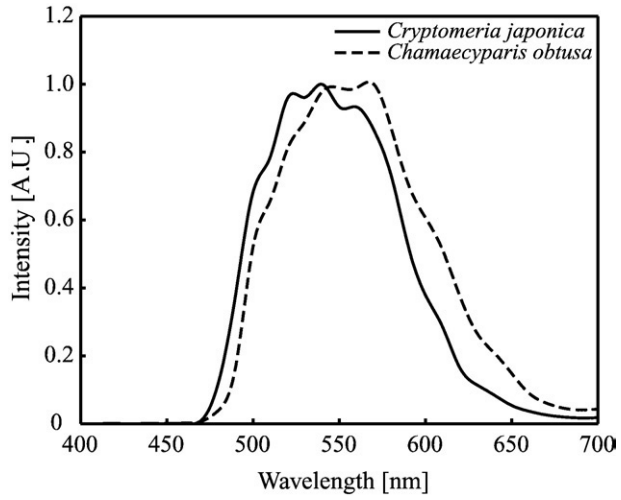

FIG. 4. Fluorescence spectra of *Cryptomeria japonica* and *Chamaecyparis obtusa* obtained using the VariSpec tunable filter and the CCD camera system.

Table 2. Pollen diameters and circularity values measured using FPIA-3000 flow image analyzer

Species	Diameter [μm]	Circularity	*n*
Cryptomeria japonica	26.0±1.56	0.99±0.01	139
Chamaecyparis obtusa	24.0±1.93	0.95±0.06	184
Dactylis glomerata	31.7±3.48	0.92±0.06	56
Ambrosia artemisiaefolia var. *elatior*	20.7±1.39	0.99±0.03	207

Each value represents the mean±SD.

a 3D volumetric fluorescence image of pollen grains obtained with a confocal laser scanning microscope (7). Although the recognition rate was as high as 90%, this method requires volumetric data sets to classify the pollen grains and does not permit real-time analysis. In comparison, the B/R ratio used in the present study is a much simpler index that can be used to classify airborne pollen grains in real time. For pollens which had similar B/R ratios, such as *F. crenata* and *B. mandshurica* var. *japonica*, the difference of grain sizes also contributed to the classification and most of pollens in this study were distinguished (Fig. 3). Even though both B/R ratio and the grain size were used, *A. artemisiaefolia* var. *elatior* and *A. princes* were not separated in the graph. These overlapped pollens could be classified clearly by the use of other parameters such as the shape of grain or the pollen season.

The B/R ratios obtained from the fluorescence images were comparable to those obtained from the pollen fluorescence spectra measured using a tunable filter. The intensity of the fluorescence images captured by the three-shot CCD camera was supposed to be affected by the characteristics of the color filters used by the camera. To minimize the effect of the color filter, we used a VariSpec camera system to measure the fluorescence spectrum. The B/R ratios of *C. japonica* and *C. obtusa* calculated using the blue and red AUCs were almost identical to the results of the image analysis. This result demonstrates that the B/R ratio obtained from the image analysis is a reliable parameter for classifying pollen grains.

Even though isopropyl alcohol would affect the condition of pollen, the pollen sizes measured by FPIA-3000 were not significantly different from those obtained using fluorescence microscopy. Accordance of the pollen size that supported the flow system is available to the automatic pollen counter. Fluorescence images showed that *C. japonica* and *A. artemisiaefolia* var. *elatior* pollen grains were spherical with a circularity of 0.99, and *D. glomerata* pollen grains were less spherical (with a circularity of 0.92). Because lower circularity values represent more complicated particle shapes that differ from true spheres, the dispersion in the data for *D. glomerata* pollen was larger than those of *C. japonica* and *A. artemisiaefolia* var. *elatior* when using the flow system (Table 2). The result of circularity suggests that the accuracy of pollen classification may be declined when the lower circularity pollens are plotted close each other in the scatter-plot.

In the field of molecular biology or pathology, the flow cytometry which measures forward and side scattered light and fluorescence is applied to analyze the character of cells in a liquid stream. Based on this technology, the instruments like a flow cytometer, but suitable for a gas stream, is the preferred choice for counting and sizing airborne particles in real time. An air-flow system enables continuous sampling and detection of aerosols simultaneously. Analytical parameters we proposed require only two fluorescence detectors; that is expected to contribute to simplification and the cost reduction of the instrument compared with an ordinary flow cytometer. Supposing that our pollen classification method is applied to the instrument, the pollen size was also measured using the particle size analyzer, which quantifies the mean size and dispersion of the particles based on diffraction and scattering of laser light in a gas stream. The results differed little from those obtained using fluorescence microscopy, indicating that the scattered-light intensity from pollen grains in a gas flow system can be applicable to a size parameter of real-time pollen classification.

In this paper, we showed the blue to red pollen autofluorescence ratio varied among the study species, as did the size of the pollen grains; and the graph of the relationship between the two parameters clearly distinguished between the pollen of the different species. An instrument based on a particle counter would be applied to real-time pollen monitoring; however, it has a difficulty to distinguish similar size pollens only by the particle size information. Our findings suggest that a flow system which measures both scattered light and the autofluorescence of the pollen could be suitable for automatically classifying and counting airborne pollen grains in real time.

ACKNOWLEDGMENTS

Two of the authors are grateful to Dr. Y. Takahashi for the supply of valuable pollen grains.

References

1. **Durham, O. C.:** The volumetric incidence of atmospheric allergens. IV. A proposed standard method of gravity sampling, counting, and volumetric interpolation of results, J. Allergy, **17,** 79–86 (1946).
2. **Hirst, J.:** An automatic volumetric spore trap, Ann. Appl. Biol., **39,** 257–265 (1952).
3. **McCrone, W. C. and Delly, J. G.:** Ultraviolet (365 nm) and blue-violet fluorescence analysis of particles, p. 857. *In* The Particle Atlas, vol. IV, Ann Arbor Science Publishers, Ann Arbor, (1973).
4. **Pinnick, R. G., Hill, S. C., Nachman, P., Pendleton, J. D., Fernandez, G. L., Mayo, M. W., and Bruno, J. G.:** Fluorescence particle counter for detecting airborne bacteria and other biological particles, Aerosol Sci. Technol., **23,** 653–664 (1995).
5. **Aronne, G., Cavuoto, D., and Eduardo, P.:** Classification and counting of fluorescent pollen using an image analysis system, Biotechnol. Histochem., **76,** 35–40 (2001).
6. **Agustin, E. F., Mark, E. W., and Robert, T. D.:** Application of fluorescence microscopy and image analysis for quantifying dynamics of maize pollen shed, Crop Sci., **42,** 2201–2206 (2002).
7. **Ronneberger, O., Schultz, E., and Burkhardt, H.:** Automated pollen recognition using 3D volume images from fluorescence microscopy, Aerobiologia, **18,** 107–115 (2002).
8. **Fricker, M. D., Chow, C. M., Errington, R. J., May, M., Mellor, J., Meyer, A. J., Tlalka, M., Vaux, D. J., Wood, J., and White, N. S.:** Quantitative imaging of intact cells and tissues by multi-dimensional confocal fluorescence microscopy, Exp. Biol. Online 2, **19,** 1–25 (1997).
9. **Terasaki, M.:** Fluorescent labeling of endoplasmic reticulum, p. 125–135. *In* Wang, Y-L. and Taylor, D. L. (eds), Fluorescence microscopy of living cells in culture, part A. Methods in Cell Biology, vol. 29, Academic Press, San Diego (1989).
10. **Mie, G.:** Beiträge zur Optik trüber Medien, speziell kolloidaler Metallösungen, Ann. Phys., **25,** 377–445 (1908).